

Flow Rates of Solid Particulate Pharmaceuticals

F. Q. DANISH* and E. L. PARROTT

Abstract □ The flow rates of particles of sodium chloride and lactose through circular orifices were measured. Equations are presented relating the flow rate (Q), diameter of the particles (D_p), and diameter of the orifice (D_o). The addition of fine particles increased the flow rate to a maximum value; then a further increase in concentration of fines caused a decrease in flow rate. For 10% fines, a decrease in particle size caused an increase in flow rate to a maximum value, after which a further size reduction resulted in a slower flow rate.

Keyphrases □ Flow rates—diameter of particles, orifice □ Particulate solids—flow rates □ Fines—maximum flow rate □ Flowometer—granulation flow rates □ Repose angle—flow rates

The flow of particulate solids is an important factor in the production of pharmaceuticals. High-speed filling machines are used to deliver a given quantity of a powder or granulation into its package. The material must flow readily and consistently to ensure the desired fill. Solid dosage forms, such as capsules, tablets, and divided powders, require measured filling for the production of each unit. The uniformity of the final product requires a uniform flow rate of the powdered or granular formulation.

A review of the literature (1-5) reveals that little is known of the basic nature of the flow of particulate solids. Flowing particulate solids do not behave as fluids or solids. The free surface of a fluid in a gravitational field is horizontal, but the surface of a particulate solid can be inclined at slopes up to its repose angle. A particulate solid must expand locally to change its shape (6). It may show deformation similar to plastic deformation of solids (7).

Most investigations (8-12) of the flow of particulate solids have been conducted on monosized systems and with apparatus of much smaller or larger dimensions than those commonly encountered in tableting and filling operations. This investigation was initiated to demonstrate a relationship between flow rate, particle size, and diameter of orifice through which the flow

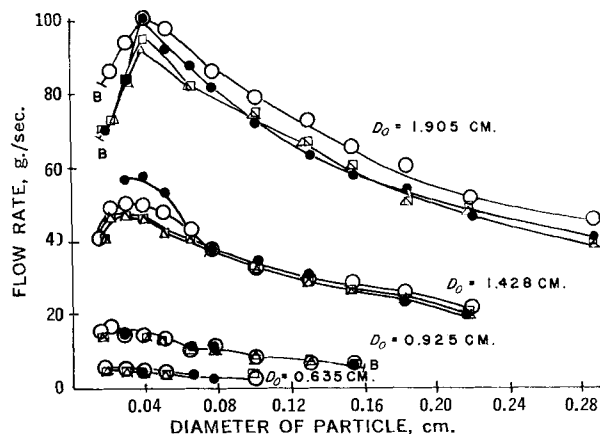


Figure 1—Influence of relative humidity on the flow rate of various sizes of sodium chloride particles through several sizes of a circular orifice. Key: ○, 0; □, 30; △, 60; and ●, 80% relative humidity; and B, blocked.

occurs. The diameters of the circular orifices were the approximate size of the flow path found in tablet presses and filling machines. The particle sizes ranged from 0.03 to 0.154 cm., which included the sizes encountered in most pharmaceutical production. The particulate solids were composed of lactose and sodium chloride. A lactose granulation prepared with starch paste was selected because it is one of the most frequently used tablet bases. Sodium chloride granules were used to represent a particulate system that may be directly compressed.

EXPERIMENTAL

Preparation of Monosized Particles—Sodium chloride¹ was milled through a No. 4 circular screen in a FitzMill with the blunt edges forward. The sodium chloride crystals were milled at slow, medium, and fast speeds to obtain an adequate quantity of various sizes required for the investigation. Five hundred grams of the milled sodium chloride was separated into size fractions by shaking for 5 min. in a Tyler sieve shaker containing appropriate U. S. standard sieves. The size fraction is expressed as a diameter which is the arithmetic mean of the openings of adjacent sieves. Size fractions larger than 0.030 cm. were treated with compressed air to remove any fine particles.

The lactose granulation containing 3% of starch was prepared by a wet granulation method. A 10% starch paste was added to the hydrous lactose USP in a Hobart mixer. After the starch paste and lactose were blended, the wet mass was passed manually through a 6-mesh screen. The wet granulation was collected on trays lined with paper and dried at 38° for 17 hr. The dried lactose granulation was then processed in the same manner as the sodium chloride.

Measurement of Flowability—The repose angle (θ) was measured by a fixed funnel and free-standing cone method (13). The reported value is the average of five determinations.

The flowometer consisted of a vertically mounted, cylindrical, stainless steel tube with an internal diameter (D_o) of 6.0 cm. and a height of 35.0 cm. A circular orifice of 1.905 cm. was accurately

Table I—Influence of Height of Fill in Flowometer on Flow Rate of 45/60-Mesh Size Fraction of Sodium Chloride through 0.635- and 0.925-cm. Circular Orifices

Initial Fill, cm.	—0.925-cm. Orifice—		—0.635-cm. Orifice—	
	Fill after Measurement, cm.	Flow Rate, g./sec.	Fill after Measurement, cm.	Flow Rate, g./sec.
6.0	3.0	14.7	4.9	5.0
9.0	6.0	14.9	7.9	5.0
12.0	9.3	15.5	10.9	5.0
15.0	12.3	14.5	14.0	4.9
18.0	15.3	14.5	17.0	4.9
21.0	18.1	14.3	20.0	4.8
24.0	21.2	14.1	23.0	4.9
27.0	24.1	14.0	26.0	4.9
30.0	27.2	14.0	29.0	4.9
33.0	30.2	14.0	32.0	4.9

¹ Sterling brine crystals, International Salt Co., Summit, Pa.

Table II—Flow Rate through a 1.905-cm. Circular Orifice and Repose Angle for Various Sizes of a Sodium Chloride and a Lactose Granulation

Mesh	Arithmetic Mean Diameter, cm.	Lactose		Sodium Chloride	
		Flow Rate, g./sec.	Repose Angle	Flow Rate, g./sec.	Repose Angle
12/14	0.1540	28.5	25.8°	—	—
14/16	0.1300	31.2	27.0°	66.6	33.2°
16/20	0.1015	34.4	28.0°	73.8	33.6°
20/25	0.0775	36.7	28.4°	82.9	32.1°
25/30	0.0650	38.6	28.8°	88.0	32.1°
30/40	0.0505	41.3	29.9°	93.8	32.8°
40/45	0.0385	42.0	30.9°	99.6	34.0°
45/60	0.0300	42.4	34.0°	101.0	35.2°
60/80	0.0213	38.8	33.9°	95.5	35.4°
80/100	0.0163	22.2	37.0°	91.3	36.6°
100/140	0.0127	21.7	37.7°	72.6	36.6°
140/200	0.0090	14.9	39.8°	Blocked	43.0°
200/325	0.0059	Blocked	42.1°	Blocked	50.6°

drilled in the center of the horizontal base plate. A spring shutter was fitted within guides on the base of the flowmeter to allow rapid operation. Circular stainless steel plates, accurately drilled with orifice diameters (D_o) of 1.428, 0.925, and 0.635 cm., could be placed in the base of the flowmeter to vary the orifice through which flow occurred.

A flat-bottom flowmeter was selected so that the particles above the orifice would flow over each other rather than on a wall as in flow from a funnel-shaped vessel. Thus, any effect of the cone angle on flow rate was eliminated, and the flow rate more closely reflected the actual flow of the particles.

When particulate solids flow from a flat-bottom container, a dead or stationary region from which particles do not flow is at the periphery of the base of the container. This influences the flow rate and is known as the wall effect. A wall effect is encountered when the ratio of the diameter of the container to the diameter (D_p) of the particles is small. A number of relationships have been suggested to describe this effect (9, 14–16). The wall effect is not significant if the difference between the diameter of the container and the diameter of the orifice is greater than 30 times the diameter of the particles, i.e., $(D_c - D_o) > 30 D_p$. Literature (8, 12, 17) shows that the flow rate is independent of the diameter of the flowmeter if $D_c/D_o > 2.5$.

The flowmeter used in this study had a diameter of 6.0 cm., so with all orifices used the wall effect was insignificant for particles smaller than 0.20 cm. in diameter.

Since the weight of a stationary and dynamic column of a particulate solid is supported by the vertical walls and not by the base of a container, the height of the column should not affect the flow rate (15, 18). The flow rate is independent of the height or head of a column of particulate solid if the head is greater than twice the diameter of the container (9, 17, 19–21). When the head of a column falls below $2.5D_c$, the flow rate is increased. The flow rates at various heights using particles of sodium chloride with a diameter of 0.030 cm. are shown in Table I for two orifices. The data show that if the height of fill remaining exceeded approximately $2.5D_c$ or 18 cm., the influence of head on the flow rate was negligible. If the height of fill remaining was less than 18 cm., the flow rate was increased until the quantity of material was insufficient to flow. Therefore, through-

out this study the height of fill remaining exceeded 18 cm. so that the influence of head on flow rate was negligible.

The flow rate was determined by collecting and weighing the material that flowed from the flowmeter in a given time. A discharge time of 6 sec. was used with orifice diameters of 1.905 and 1.428 cm.; a discharge time of 12 sec. was used with orifice diameters of 0.925 and 0.635 cm. The flow rate (Q) is expressed in grams discharged per second. The reported flow rate is the average of five determinations. The variation of the flow rate did not exceed 5%.

Humidity—A high moisture content is known to reduce the flowability of some granular materials (22). To determine the influence of humidity on the flow of sodium chloride particles, they were exposed for 36 hr. to 0, 30, 60, and 80% relative humidity (23). The moisture content was determined with an Ohaus moisture balance; it did not exceed 0.4%. As shown in Fig. 1, at low and moderate humidities the effect of humidity on the flow rate of particles of sodium chloride was not significant. At 80% relative humidity, the particles tended to cake, but they flowed after shaking.

The moisture content of the lactose granulation after exposure to 60% relative humidity did not exceed 0.4%. It has been reported that lactose below 65% relative humidity contains negligible moisture (24) and remains free flowing (25).

Because the flow of sodium chloride and lactose particles was not affected by the humidities in the laboratory, no further effort was made to control humidity. All measurements were made at ambient humidity and temperature.

RESULTS AND DISCUSSION

Repose Angle and Flow Rate—Angular properties have been used to classify powders and granules; however, a relationship between an angular property and flow rate has not been expressed (22, 26–28). The flow rate and repose angle of various size fractions of lactose and sodium chloride are given in Table II and are plotted in Figs. 2 and 3. The results support the conclusion of Gold *et al.* (29) that there is no correlation between actual flow properties and repose angle.

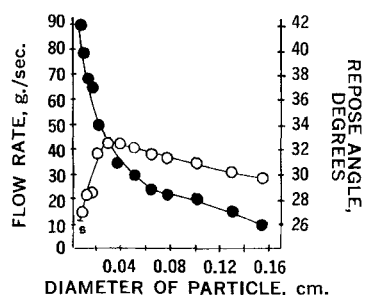


Figure 2—Flow rate through a 1.905-cm. circular orifice and repose angle for various sizes of lactose granulation. Key: ○, flow rate; ●, repose angle; and B, blocked.

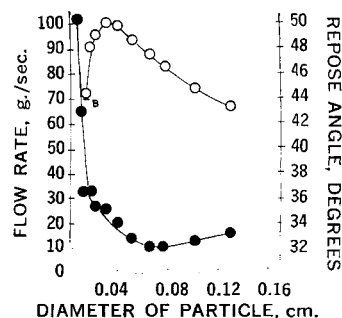


Figure 3—Flow rate through a 1.905-cm. circular orifice and repose angle for various sizes of sodium chloride particles. Key: ○, flow rate; ●, repose angle; and B, blocked.

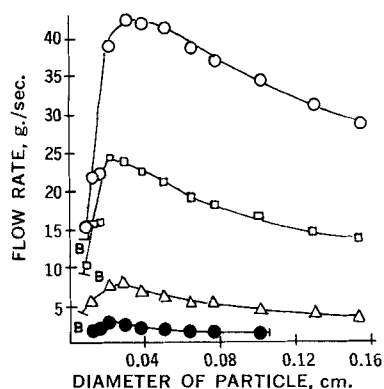


Figure 4—Flow rate of various sizes of lactose granulation through circular orifices with diameters: ○, 1.905; □, 1.428; △, 0.9250; ●, 0.6530 cm.; and B, blocked.

Since active flow is an important factor in pharmaceutical manufacturing, it seems valid to characterize particulate solids in a dynamic term. Because the repose angle expresses static interparticulate friction, it was decided to study the flow of particulate solids by means of a flowometer, which measures a dynamic flow rate that closely simulates the actual production conditions.

The most important single factor controlling flow rate is the diameter of the orifice (8, 30). As shown in Figs. 1 and 4, the flow rate is increased as the diameter of the orifice is increased. The flow rate is proportional to a power of the diameter of the orifice. The power may be empirically evaluated by a plot of $\log Q$ against $\log D_o$ (15, 31, 32). The linear relationship of $\log Q$ to $\log D_o$ for lactose and sodium chloride is shown in Figs. 5 and 6.

Figures 1 and 4 show that for a given orifice the flow rate is increased to a maximum rate as the particle size is decreased and that a further reduction of particle size results in a slower flow rate. For both materials the maximum flow rate through various orifices occurred when the particles were 0.03 cm. in diameter.

Relation of Q , D_p , and D_o —Brown and Richards (33), in their examination of the empty annulus adjacent to the edge of an orifice, developed an equation for the purpose of finding the orifice giving rise to zero flow. The equation is:

$$(4Q/\pi\rho\sqrt{g})^{0.4} = mD_o + C \quad (\text{Eq. 1})$$

where Q is the flow rate in grams per second, ρ is the density of the material, g is the acceleration of gravity, and m and C are constants. Figures 7 and 8 are plots of the equation using experimental values for monosized particles of lactose and sodium chloride. The constants m and C may be evaluated from the slope and intercept with the ordinate axis, respectively, of this linear plot. Attempts (15, 34–36) have been made to relate bulk density to flow rates; however, it is doubtful if any arbitrarily selected bulk density can be correlated with flow because a particulate solid expands with a decrease in

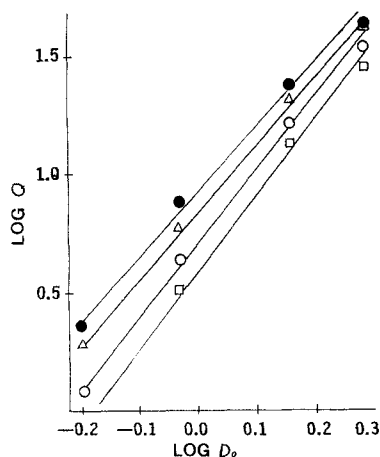


Figure 5—Log-log relationship of diameter of circular orifice to the flow rate of lactose granulation of various particle size. Key: □, 0.1540; ○, 0.1015; △, 0.0505; and ●, 0.0300 cm.

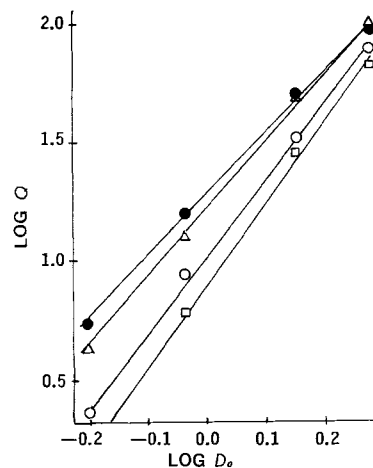


Figure 6—Log-log relationship of diameter of circular orifice to the flow rate of sodium chloride granules of various size. Key: □, 0.1540; ○, 0.1015; △, 0.0505; and ●, 0.0300 cm.

density when it begins to flow (12, 37). Thus, rather than select some bulk density, which is not representative of the density of the flowing particles, the density of the material was used (19).

Upon rearrangement of Eq. 1 and substitution of $k = -C/m$,

$$D_o = 1/m(4Q/\pi\rho\sqrt{g})^{0.4} + k \quad (\text{Eq. 2})$$

The general use of the equation of Brown and Richards (33) is supported by Jones and Pilpel (38) and this study. The relationship applies in the region where a decrease in particle size causes an increase in flow rate. When the particle diameter is less than 0.025 cm., other forces, which were discussed by Jones and Pilpel (39), influence the flow rate. In pharmaceutical operations involving flow of particulate solids, the sizes of the particles are usually larger than 0.059 cm. For these reasons the present investigation was restricted to particles with a diameter larger than 0.025 cm.

The intercept with the ordinate axis and the slope of each straight line in Fig. 8 were determined. A plot of the reciprocal ($1/m$) of the slope of each particle size against D_p is linear and is expressed by the relationship

$$1/m = 0.75D_p + 1.36 \quad (\text{Eq. 3})$$

A plot of $\log k$ against $\log D_p$ is linear and can be used to evaluate the constants for the relationship.

$$k = 1.202D_p^{0.768} \quad (\text{Eq. 4})$$

Upon the substitution of $1/m$ from Eq. 3 and k from Eq. 4 into Eq. 2,

$$D_o = (1.36 + 0.75D_p)(4Q/\pi\rho\sqrt{g})^{0.4} + 1.202D_p^{0.768} \quad (\text{Eq. 5})$$

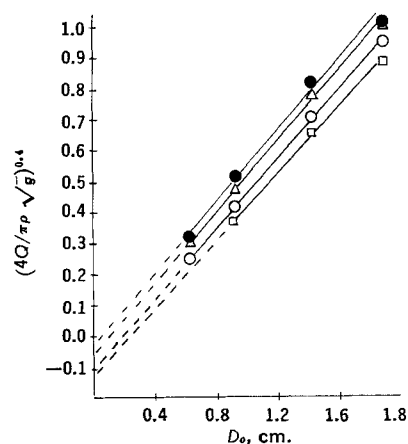


Figure 7—Influence on relationship of $(4Q/\pi\rho\sqrt{g})^{0.4}$ to diameter of orifice of lactose granulation of various particle size. Key: □, 0.1540; ○, 0.1015; △, 0.0505; and ●, 0.0300 cm.

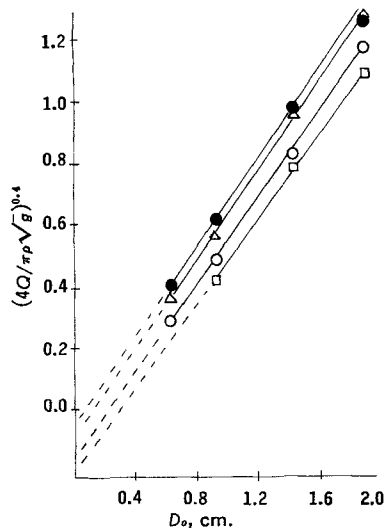


Figure 8—Influence on relationship of $(4Q/\pi\rho\sqrt{g})^{0.4}$ to diameter of orifice of sodium chloride granules of various particle size. Key: \square , 0.1540; \circ , 0.1015; \triangle , 0.0505; and \bullet , 0.0300 cm.

After rearrangement, the flow rate of particles of sodium chloride is related to the diameter of the orifice and the diameter of the particles by the equation

$$Q = [(D_o - 1.202D_p^{0.768})/(1.36 + 0.75D_p)]^{2.5}(\pi\rho\sqrt{g}/4) \quad (\text{Eq. 6})$$

Adjacent to the periphery of the orifice, there is an empty space or annulus with a width ($k/2$) that is independent of the size of the orifice (19, 33, 35, 40). Thus, the effective diameter of a circular orifice is $(D_o - k)$. If Eq. 2 is written

$$D_o - k = 1/m(4Q/\pi\rho\sqrt{g})^{0.4} \quad (\text{Eq. 7})$$

it is readily seen that the flow rate is a function of the effective diameter of the orifice. When $(4Q/\pi\rho\sqrt{g})^{0.4}$ is plotted against the effective diameter, a straight line passing through the origin is produced (Fig. 9). The relation of this function of flow rate to effective diameter of the orifice is constant regardless of particle size. Therefore, the statement that flow rate is a function of particle size requires qualification. The flow rate in the actual region of movement of particles is independent of particle size. Flow is affected by particle size only to the extent that particle size changes the value of k .

It may be more practical to use the measured diameter (D_o) than the effective orifice diameter, which requires the evaluation of k . Since k is a function of D_p , Eq. 2 may be written

$$D_o = 1/m(4Q/\pi\rho\sqrt{g})^{1/n} \quad (\text{Eq. 8})$$

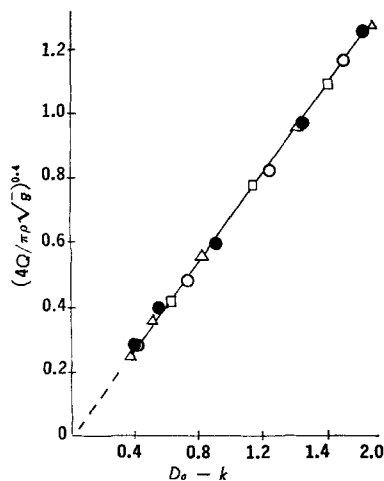


Figure 9—Relationship of $(4Q/\pi\rho\sqrt{g})^{0.4}$ to effective diameter of the orifice for various particle size. Key: \square , 0.1540; \circ , 0.1015; \triangle , 0.0505; and \bullet , 0.0300 cm.

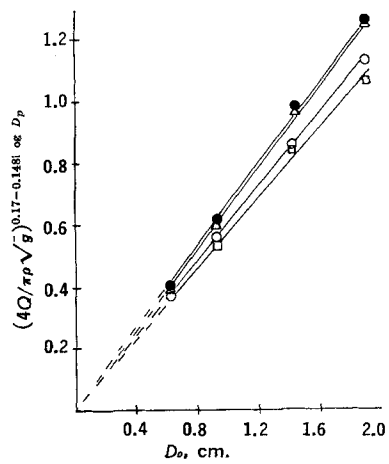


Figure 10—Influence on relationship of $(4Q/\pi\rho\sqrt{g})^{0.17 - 0.148 \log D_p}$ to diameter of orifice for sodium chloride granules of various particle size. Key: \square , 0.1540; \circ , 0.1015; \triangle , 0.0505; and \bullet , 0.0300 cm.

where $1/m$ and $1/n$ are functions of particle size. If the reciprocals of the slopes of the plot of $\log Q$ against $\log D_o$ in Fig. 5 are plotted against $\log D_p$, there is a linear relationship, which may be expressed

$$1/n = 0.17 - 0.148 \log D_p \quad (\text{Eq. 9})$$

Substitution of Eq. 9 into Eq. 8 gives

$$D_o = 1/m(4Q/\pi\rho\sqrt{g})^{0.17 - 0.148 \log D_p} \quad (\text{Eq. 10})$$

When the experimental data are used in Fig. 10 to plot $(4Q/\pi\rho\sqrt{g})^{0.17 - 0.148 \log D_p}$ against D_o , a straight line, which passes through the origin, is produced. The slopes of these lines are used to relate Q , D_o , and D_p . For each particle size, the reciprocal of the slope was plotted against D_p to evaluate the constants for the relationship

$$1/m = 1.41 + 2.5D_p \quad (\text{Eq. 11})$$

Upon substitution of $1/m$ from Eq. 11 into Eq. 10 and rearrangement,

$$Q = [D_o/(1.41 + 2.5D_p)]^{1/(0.17 - 0.148 \log D_p)}(\pi\rho\sqrt{g}/4) \quad (\text{Eq. 12})$$

which is equivalent to Eq. 6 for particles of sodium chloride.

The constants for the lactose granulation were evaluated in a similar manner; however, to conserve space only Eqs. 13 and 14 and Figs. 7 and 11 are presented:

$$Q = [(D_o - 1.202D_p^{0.781})/(1.72 + 0.757D_p)]^{2.5}(\pi\rho\sqrt{g}/4) \quad (\text{Eq. 13})$$

$$Q = [D_o/(1.677 + 2.11D_p)]^{1/(0.243 - 0.08 \log D_p)} \times (\pi\rho\sqrt{g}/4) \quad (\text{Eq. 14})$$

The comparison of the experimental and calculated flow rates in

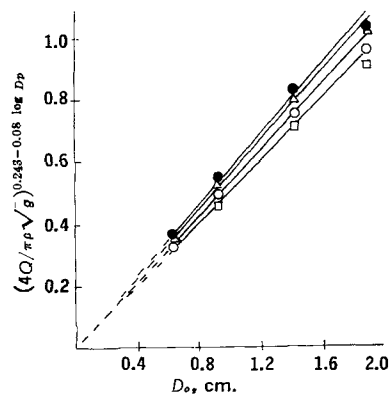


Figure 11—Influence on relationship of $(4Q/\pi\rho\sqrt{g})^{0.243 - 0.08 \log D_p}$ to diameter of orifice for lactose granulation of various size. Key: \square , 0.1540; \circ , 0.1015; \triangle , 0.0505; and \bullet , 0.0300 cm.

Table III—Experimental Rate (Q) and Calculated Rate ($Q_{\text{calcd.}}$) of Flow through a 1.428-cm. Circular Orifice for Various Monosized Particles

Mesh	Size, cm.	Q , g./sec.	$Q_{\text{calcd.}}$, g./sec.	Error, %	$Q_{\text{calcd.}}$, g./sec.	Error, %
Lactose		Experimental	Equation 13		Equation 14	
12/14	0.1540	13.5	12.1	-9.5	13.0	-2.4
14/16	0.1300	14.5	13.3	-7.8	14.4	-0.3
16/20	0.1015	16.4	15.0	-9.3	16.3	-0.3
20/25	0.0755	17.9	16.8	-6.1	18.3	2.4
25/30	0.0650	18.9	17.6	-7.1	19.2	1.5
30/40	0.0505	20.7	18.7	-9.3	20.6	-0.6
40/45	0.0385	22.3	19.8	-11.2	21.8	-2.5
45/60	0.0300	23.9	20.6	-13.7	22.7	-5.0
Sodium Chloride		Experimental	Equation 6		Equation 12	
8/10	0.2190	21.2	21.1	-0.1	16.3	-22.6
10/12	0.1840	25.3	24.6	-2.1	20.2	-20.2
12/14	0.1540	28.6	28.0	-1.9	24.2	-15.4
14/16	0.1300	30.0	31.1	3.6	27.8	-7.0
16/20	0.1015	32.7	35.4	8.3	32.9	0.4
20/25	0.0755	38.3	39.5	3.3	37.9	-0.8
25/30	0.0650	42.4	41.9	-1.0	40.3	-4.9
30/40	0.0505	47.9	45.0	-6.2	43.5	-9.2
40/45	0.0385	49.8	47.7	-4.1	46.2	-7.1
45/60	0.0300	49.8	49.8	0	48.2	-3.1

Table III demonstrates the validity of Eqs. 6 and 12 for monosized particles of sodium chloride and of Eqs. 13 and 14 for monosized particles of lactose granulation. Similar comparisons for other orifices show that, in general, the value of the calculated and experimental flow rates are within a 10% variation.

Because real particulate solids are composed of various sizes of particles, it would be useful to have an equation that could be applied to calculate the flow rates of polysized particulate solids. Following the pattern of Jones and Pilpel (38), binary and ternary mixtures were prepared, and the flow rates were measured. The particle diameter ($D_{pav.}$) of the mixture was represented by the geometric mean diameter, e.g., for a binary mixture

$$D_{pav.} = \sqrt{D_{p_1}^{m_1/0.5} \times D_{p_2}^{m_2/0.5}} \quad (\text{Eq. 15})$$

where m_1 and m_2 are the weight fractions of particles of diameter D_{p_1} and D_{p_2} , respectively.

In applying Eqs. 13 and 14 for monosized particles to the calculation of flow rates of mixtures of lactose, it was found that the best correlation between experimental and calculated flow rate was obtained if the right side of the equation was multiplied by an empirical factor of 1.14. Thus, for mixtures of the lactose granulation,

$$Q = 1.14 [(D_o - 1.202D_{pav.}^{0.781}) / (1.72 + 0.757D_{pav.})]^{2.5} \times (\pi\rho\sqrt{g}/4) \quad (\text{Eq. 16})$$

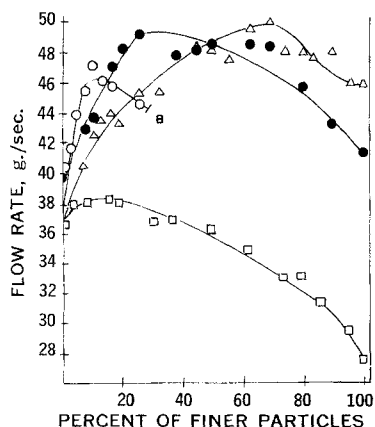


Figure 12—Influence of percent of fine particles of sodium chloride on the flow rate through a 1.428-cm. circular orifice of 16/20-mesh size fraction of sodium chloride. Key to diameter of fine particle: ○, 0.0090; ●, 0.0163; △, 0.0385; □, 0.1540 cm; and B, blocked.

and

$$Q = 1.14 [D_o / (1.677 + 2.11D_{pav.})]^{1/(0.243 - 0.68 \log D_p)} \times (\pi\rho\sqrt{g}/4) \quad (\text{Eq. 17})$$

The calculated flow rates using Eqs. 16 and 17 for binary and ternary mixtures of lactose granulation are compared to the experimental flow rates in Tables IV and V.

Similarly, for sodium chloride particles, the flow rate of the mixtures may be expressed by multiplying the right side of Eqs. 6 and 12 by the factor of 1.14 so that for mixtures:

$$Q = 1.14 [(D_o - 1.202D_{pav.}^{0.768}) / (1.36 + 0.75 D_{pav.})]^{2.5} \times (\pi\rho\sqrt{g}/4) \quad (\text{Eq. 18})$$

$$Q = 1.14 [D_o / (1.41 + 2.5D_{pav.})]^{1/(0.17 - 0.148 \log D_{pav.})} \times (\pi\rho\sqrt{g}/4) \quad (\text{Eq. 19})$$

In general, for both materials the experimental and calculated flow rates of binary and ternary mixtures using these equations are within a 10% variation.

The bulk density of a polysized particulate bed is greater than that of a monosized system because the smaller particles tend to fill the void between the larger particles. Similarly, in a flowing polysized particulate system the smaller particles fit within the void between the larger particles. Consequently, there is a greater mass of material per unit volume of discharge and there is a greater flow rate. Thus, the factor 1.14 may be considered as a correction for the increased bulk density of the polysized system during actual flow.

Fines—The influence of fine particles on the flow rate of larger particles was demonstrated by the addition of finer, monosized

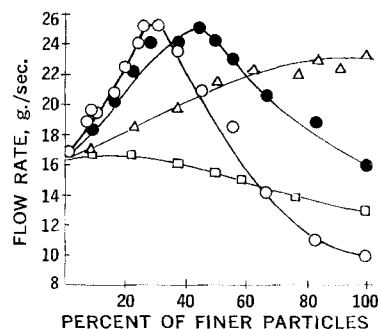


Figure 13—Influence of percent of fine particles of lactose granulation on the flow rate through a 1.428-cm. circular orifice of 16/20-mesh size fraction of lactose granulation. Key to diameter of fine particle: ○, 0.0090; ●, 0.0163; △, 0.0385; and □, 0.1540 cm.

Table IV—Experimental Rate (Q) and Calculated Rate ($Q_{\text{calcd.}}$) of Flow through a 1.428-cm. Circular Orifice for Binary Mixtures of Monosized Particles of Lactose Using Eqs. 16 and 17

D_{p1} , cm.	Percent	D_{p2} , cm.	Percent	Q , g./sec.	Equation 16		Equation 17	
					$Q_{\text{calcd.}}$, g./sec.	Error, %	$Q_{\text{calcd.}}$, g./sec.	Error, %
0.1015	75	0.1540	25	16.5	16.4	-0.6	17.7	7.8
	50		50	15.3	15.5	1.6	16.8	10.1
	25		75	13.9	14.7	5.8	15.9	14.4
0.1015	75	0.0385	25	18.5	18.5	1.8	20.5	11.1
	50		50	21.4	20.3	-5.1	22.2	3.8
	25		75	22.4	21.5	-3.6	23.6	5.7
0.1015	75	0.0163	25	22.4	20.1	-9.9	22.0	-1.5
	50		50	24.1	22.4	-6.9	24.0	2.1
	25		75	19.2	24.0	25.3	26.5	38.0

Table V—Experimental Rate (Q) and Calculated Rate ($Q_{\text{calcd.}}$) of Flow through a 1.428-cm. Circular Orifice for Ternary Mixtures of Monosized Particles of Lactose Using Eqs. 16 and 17

Percent of			Q , g./sec.	Equation 16		Equation 17	
0.1015	D_p , cm. 0.0650	0.0127		$Q_{\text{calcd.}}$, g./sec.	Error, %	$Q_{\text{calcd.}}$, %	Error, %
25	50	25	25.0	21.7	-13.0	23.8	-4.5
33.3	33.3	33.3	24.4	22.0	-9.6	24.2	-0.7
50	25	25	23.2	21.2	-8.6	23.2	-0.5
25	25	50	24.1	23.4	-2.9	25.7	6.7

particles to particles with a diameter of 0.1015 cm. After blending for 5 min. in a V-blender, the flow rate was measured. As the concentration of the finer particles was increased and more of the void between the larger particles was filled, the flow rate was increased to a maximum value; then as a greater concentration was added, the flow rate was decreased.

As shown in Fig. 12, the smallest size of the finer particles required the lowest concentration of the finer particles to obtain the maximum flow rate. For example, maximum flow rates of particles with a diameter of 0.1050 cm. were obtained upon the addition of 9.9, 25.9, and 69% of fine particles with diameters of 0.0090, 0.0163, and 0.0385 cm., respectively. Although a maximum flow rate was obtained at a lower concentration of the finest particles, the value of the maximum flow rate may be less than the maximum flow rate obtained upon the addition of a greater concentration of a larger-sized fine particle. For example, the addition of 9.9% of fine particles with a diameter of 0.0090 cm. to particles with a diameter of 0.1050 cm. produced a maximum flow rate of 47.1 g./sec., while the addition of 25.9% of fine particles with a diameter of 0.0163 cm. produced a maximum flow rate of 49.3 g./sec.

As shown in Fig. 13, for the lactose granulation having a diameter of 0.1050 cm., maximum flow rates were 25.2, 25.2, and 22.3 g./sec. upon the addition of 25.9% of particles having a diameter of 0.0090

cm., 44.4% of particles having a diameter of 0.0163 cm., and 62.5% of particles having a diameter of 0.0385 cm., respectively.

The influence of the size of fine particles on the flow rate of particles of sodium chloride and lactose with a diameter of 0.1050 cm. by the addition of 10% fines is shown in Fig. 14. As the diameter of the finer particles was decreased to 0.009 cm., the flow rate was increased because the weight per unit volume of flow was greater. When the diameter is less than 0.009 cm. and the void space is mostly filled by the smaller particles, it appears that the number of points of contact is so large that interparticle friction becomes great enough to slow the flow rate.

SUMMARY

1. A flowmeter was used to study the flow of a sodium chloride and a lactose granulation through a circular, horizontal orifice.
2. Equations are presented relating the flow rate, diameter of the particles, and diameter of the orifice through which flow of monosized particles occurs.
3. An empirical factor is introduced into these equations so that they may be applied to binary and ternary blends of various monosized particles.
4. The addition of fine particles to a monosized particulate solid increased the flow rate to a maximum value; then as a greater concentration of fines was added, the flow rate was decreased.
5. For a given concentration of fines, the flow rate was increased to a maximum rate as the diameter of the fines was decreased to approximately 90 μ ; then further reduction in diameter of the fines resulted in slower flow rates.

REFERENCES

- (1) B. S. Neuman, in "Advances in Pharmaceutical Sciences," vol. 2, H. S. Bean, A. H. Beckett, and J. E. Carless, Eds., Academic, New York, N. Y., and London, England, 1967.
- (2) R. L. Brown and P. G. W. Hawksley, *Times Sci. Rev.*, **6**, 12(1954).
- (3) R. L. Brown and J. C. Richards, *Mon. Bull. Brit. Coal Util. Res. Ass.*, **22**, 359(1958).
- (4) J. C. Richards, *ibid.*, **19**, 145(1955).
- (5) E. N. Hiestand, *J. Pharm. Sci.*, **55**, 1325(1966).
- (6) R. L. Brown and P. G. W. Hawksley, *Fuel*, **26**, 195(1947).
- (7) A. Nadai, "Theory of Flow and Fracture of Solids," vol. 1, McGraw-Hill, New York, N. Y., 1950.
- (8) M. S. Ketchum, "The Design of Walls, Bins and Grain Elevators," 3rd ed., McGraw-Hill, New York, N. Y., 1925.

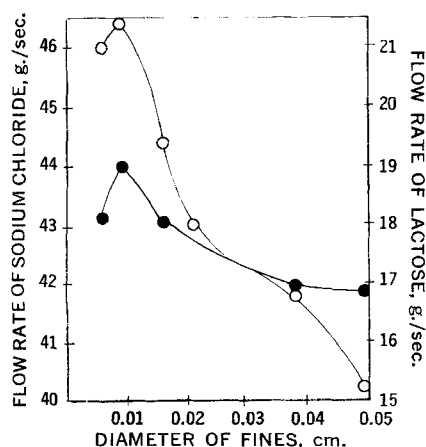


Figure 14—Influence of size of fines on the flow rate through a 1.428-cm. circular orifice of 16/20-mesh size fraction when the percent of fines is maintained at 10%. Key: \circ , sodium chloride; and \bullet , lactose granules.

- (9) E. J. Crosby, *Amer. Perfum.*, **75**, 43(1960).
 (10) H. W. Jenike, *Chem. Eng.*, **61**, 175(1954).
 (11) H. W. Jenike, *Eng. Mining J.*, **156**, 83(1955).
 (12) R. L. Brown and J. C. Richards, *Trans. Inst. Chem. Eng.*, **37**, 108(1959).
 (13) E. L. Parrott, *Amer. J. Pharm. Educ.*, **30**, 205(1966).
 (14) N. J. Pilpel, *Chem. Process Eng.*, **46**, 167(1965).
 (15) F. C. Franklin and L. N. Hohanson, *Chem. Eng. Sci.*, **4**, 119(1955).
 (16) F. A. Zenz, *Petrol. Refiner*, **36**, 162(1957).
 (17) H. E. Rose and T. Tanaka, *Engineer*, **208**, 46(1959).
 (18) J. H. Shaxby and J. E. Evans, *Trans. Faraday Soc.*, **19**, 60(1923).
 (19) A. Harmens, *Chem. Eng. Sci.*, **18**, 297(1963).
 (20) A. W. Jenike, *Trans. Inst. Chem. Eng.*, **40**, 264(1962).
 (21) I. R. McGougull and A. E. Evans, *Rheol. Acta*, **4**, 218(1965).
 (22) D. J. Craik and B. F. Miller, *J. Pharm. Pharmacol.*, **10**, 136T(1958).
 (23) A. Wexler and W. G. Prombacker, *Nat. Bur. Stand. Circ.*, **1958**, 512.
 (24) E. Shotton and N. Harb, *J. Pharm. Pharmacol.*, **17**, 504(1965).
 (25) *Ibid.*, **18**, 175(1966).
 (26) D. Train, *J. Pharm. Pharmacol.*, **10**, 127T(1958).
 (27) E. Nelson, *J. Amer. Pharm. Ass., Sci. Ed.*, **44**, 435(1955).
 (28) R. L. Carr, Jr., *Chem. Eng.*, **72**, 69(1965).
 (29) G. Gold, R. N. Duvall, B. T. Palermo, and J. G. Slater, *J. Pharm. Sci.*, **55**, 1291(1966).
 (30) R. H. Newton, G. S. Dunham, and T. P. Simpson, *Trans. Amer. Inst. Chem. Eng.*, **41**, 218(1945).
 (31) W. E. Deming and A. L. Mehring, *Ind. Eng. Chem.*, **21**, 661(1929).
 (32) R. N. Langmaid and H. E. Rose, *J. Inst. Fuel*, **30**, 166(1957).
 (33) R. L. Brown and J. C. Richards, *Trans. Inst. Chem. Eng.*, **38**, 243(1960).
 (34) K. Takahasi, *Geogr. Mag. Tokyo*, **11**, 165(1937).
 (35) K. Wieghardt, *Ing. Arch.*, **20**, 109(1952).
 (36) R. T. Fowler and J. R. Glastonbury, *Chem. Eng. Sci.*, **10**, 150(1959).
 (37) J. W. Delaplaine, *A. E. Chem. Eng. J.*, **2**, 127(1956).
 (38) T. M. Jones and N. Pilpel, *J. Pharm. Pharmacol.*, **18**, 81(1966).
 (39) *Ibid.*, **18**, 429(1966).
 (40) W. A. Beverloo, H. A. Leniger, and J. Van de Velde, *Chem. Eng. Sci.*, **15**, 260(1961).

ACKNOWLEDGMENTS AND ADDRESSES

Received October 5, 1970, from the College of Pharmacy, University of Iowa, Iowa City, IA 52240

Accepted for publication November 20, 1970.

Abstracted in part from a dissertation submitted by F. Q. Danish to the Graduate College, University of Iowa, in partial fulfillment of the Doctor of Philosophy degree requirements.

* Present address: School of Pharmacy, Creighton University, Omaha, NE 68102

Synthesis, Antileukemic Activity, and Stability of 3-(Substituted-Triazeno)pyrazole-4-carboxylic Acid Esters and 3-(Substituted-Triazeno)pyrazole-4-carboxamides

Y. FULMER SHEALY and C. ALLEN O'DELL

Abstract □ Representative 3-triazeno derivatives of the ethyl and methyl esters of pyrazole-4-carboxylic acid and of pyrazole-4-carboxamide were synthesized from the corresponding 3-diazopyrazoles. It was shown that certain triazeno-pyrazoles in solution are decomposed by light, and transformations of 3-(3-methyl-1-triazeno)pyrazole-4-carboxamide and 3-[3,3-bis(2-chloroethyl)-1-triazeno]pyrazole-4-carboxamide in solution in the dark to 3-aminopyrazole-4-carboxamide and to a *v*-triazolinium salt, respectively, were observed. All of these transformations are analogous to reactions of triazenoimidazoles observed previously. Triazeno-pyrazoles having both the ester and the amide groups increased the average survival time in the standard mouse L-1210 leukemia assay. In some of these tests, increases in lifespan of 60–120% were observed.

Keyphrases □ Triazeno-pyrazoles—synthesis, decomposition by light □ Leukemia L-1210 inhibition—triazeno-pyrazoles □ Antileukemic activity—triazeno derivatives of pyrazole esters, amides □ Diazopyrazole esters—antimicrobial activity

Various triazenoimidazolecarboxamides (*Ia*) (1–5) and triazenoimidazolecarboxylates (*Ib*) (6, 7) have been synthesized, and a number of these have displayed antineoplastic activity (2, 3, 5–10). Several triazeno-*v*-triazoles (e.g., *II*) were prepared as ring analogs of the imidazoles, and activity was also found among derivatives of this ring system (11). It seemed logical, therefore,

to extend these studies to related heterocycles. The synthesis and antileukemic activity of 3-(substituted-triazeno)pyrazole-4-carboxylic acid esters (V–VIII) and 3-(substituted-triazeno)pyrazole-4-carboxamides (X–XIV) are described in the present report. The bis(2-fluoroethyl)triazeno-pyrazoles (IX and XV) comprised part of a recent communication (12); after most of this work had been completed, one of the other derivatives, the dimethyltriazeno derivative (X) of the amide series, was reported by Noell and Cheng (13). The dimethyl-triazeno derivative of antipyrine, a pyrazolone, was prepared by Stolz (14) in 1908.

The triazeno-pyrazoles (V–XV) were prepared by the methods utilized for the synthesis of triazenoimidazoles (*I*), namely, by isolating a diazopyrazole and treating it in nonaqueous media with the appropriate amine or by diazotizing the aminopyrazole and then adding the amine to the aqueous solution without isolating the intermediate diazo derivative. Both methods afforded the simple dialkyltriazeno-pyrazolecarboxylate esters (V–VIII). The first method was used in syntheses, or attempted syntheses, of unstable triazenes, such as bis(2-haloethyl)triazeno derivatives and the mono-methyltriazene (XIII); it is preferable for the preparation of triazeno-pyrazolecarboxamides because of the competing intramolecular cyclization reaction to 3,7-